OPTIMIZATION OF UNDULATORY FLAP PROPULSORS

Jason I. Martin
Laurens E. Howle
Department of Mechanical Engineering and Materials Science
Center for Nonlinear and Complex Systems
Edmund T. Pratt Jr. School of Engineering
Duke University
Durham, NC 27708-0300
919-660-5331
laurens.howle@duke.edu

LCDR Mark M. Murray
Mechanical Engineering Department
United States Naval Academy
Annapolis, MD 21402
410-293-6451
mmmurray@usna.edu

Abstract:

This project involves analysis leading to the optimization of flap propulsors for underwater propulsion applications. Specifically, we apply our model to Pilotfish, an Unmanned Underwater Vehicle (UUV) developed by Nekton Research, LLC. We analyze the performance of the propulsors utilizing an unsteady three-dimensional vortex ring method. We set the actuation axis of the non-deforming propulsor and pitch the foils with a sinusoidal forcing function. This undulatory motion produces thrust via unsteady vortex shedding. Our present modeling involves a whole-system analysis of the unmanned underwater vehicle including the blunt hull. The blunt body produces a highly perturbed flow region near the flap propulsors. We show that this perturbed flow region alters the performance of the propulsors. Therefore, geometric optimization the flap propulsors needs to properly account for the effects of the blunt hull.

Introduction

There has been a significant amount of work on the study of oscillating propulsors (Anderson *et al.* (1998), Dickinson (1994), Murray & Howle (2001)), particularly in the study and modeling of the propulsive mechanisms of fish and other aquatic creatures (Triantafyllou *et al.* (2000), Sfakiotakis *et al.* (1999), Kagemoto *et al.* (2000), Anderson & Kerrebrock (1997)). Undulatory flap propulsion may offer several advantages over traditional propellers, including ease of thrust vector reorientation, exceptional acceleration/deceleration characteristics, and stealth.

Figure 1 - Pilotfish. The Pilotfish was constructed by Nekton Research, LLC. It uses four flap propulsors to propel itself through the water and is remotely operated by an outside user. The Pilotfish has excellent acceleration and deceleration capabilities, as it is capable of coming to a complete stop from full speed in a tenth of its body length.

One device, which takes advantage of oscillating propulsor technology, is the Pilotfish. The Pilotfish is a highly maneuverable underwater vehicle built by Nekton Research, LLC as a technology concept demonstration vehicle. The Pilotfish vehicle maximizes its maneuverability by utilizing four undulatory propulsors protruding radialy from the centroid of the elongated ellipsoidal hull in an X-configuration (Hobson et al. (1999)). Overall vehicle maneuverability is enhanced by the ease of individual propulsor thrust vector reorientation and exceptional acceleration/deceleration characteristics. Figure 1 shows the Pilotfish vehicle being prepared for testing.

The current fin (Figure 2) has been analyzed using numerical modeling methods, but the analysis was performed without taking into account the effect of the flow perturbation caused the presence of the blunt body.

Figure 2 - Fin Flap Propulsor. Shown here is one of the fin flap propulsors mounted on the side of the Pilotfish. The fin is constructed of a polyurethane elastomer and was cast by Nekton Research, LLC.

There are several parameters with which we are concerned as we optimize the performance of the flap propulsors. The actuation schedule, the planform, and the physical properties of the material from which the propulsors are constructed are the focus of our optimization efforts. However, before performing such an optimization, we would like to extend our previous model to include the flow-distorting effect produced by the hull and by the other propulsors

Mathematical Model

In this section, we discuss the mathematical model that accounts for the whole-vehicle simulation of the pilotfish including flap-hull interactions and time dependent thrust generation. We model the propulsors as two-dimensional rigid plates. Because the flap chord-wise and span-wise directions are much larger than the flap thickness, this assumption is justified and considerably simplifies our computational effort.

We assume the fluid is incompressible, irrotational and inviscid. By making these assumptions we can utilize the potential flow model. The model describes the fluid flow as the following:

$$\nabla^2 \Phi = 0 \quad (1)$$

where Φ is the scalar velocity potential the gradient of which is the velocity.

In order to solve the potential equation, we must select a singularity element. We elect to discritize the pilotfish surface using vortex ring singularity elements. Each vortex ring is composed of a quadrilateral as shown in Figure 3. The velocity induced at a point by a vortex line segment with strength Γ can be written as follows: Let the respective symbols r_0, r_1 and r_2 denote the position vectors of the point at which the induced velocity is to be calculated (not on the vortex line segment), the beginning of the straight vortex line segment and the end of the vortex line segment. Then the induced velocity components are

$$\begin{aligned} u &= K(r_1 \times r_2) \cdot i \\ v &= K(r_1 \times r_2) \cdot j \\ w &= K(r_1 \times r_2) \cdot k \end{aligned} \quad (2)$$

where the kernel, K, in equation (2) is

$$K = \frac{\Gamma}{4p\,|r_1 \times r_2|^2}\left(\frac{r_0 \cdot r_1}{r_1} - \frac{r_0 \cdot r_2}{r_2}\right). \quad (3)$$

Since a vortex line segment cannot begin or end in a fluid, we must connect several vortex line segments in order to form a closed vortex ring. The velocity induced at a point not on any segment of the vortex ring is then the summation of the velocity induced by all segments comprising the ring. Further, all segments in the same vortex ring must have the same strength, Γ.

Next, we place a collation point near the centroid of each vortex ring. At each collocation point we enforce the boundary condition

$$\left(\nabla\Phi_\infty + \nabla\Phi_B + \nabla\Phi_w - \vec{v}_{rel}\right) \cdot \hat{n} = 0 \quad (4)$$

which states that the normal component of the total velocity must vanish on the surface. In equation (4), $\nabla\Phi_\infty$ is the free-stream velocity, $\nabla\Phi_B$ is the velocity induced at the vortex rings, $\nabla\Phi_w$ is the wake-induced velocity and $\vec{v}_{rel}$ is the velocity of the surface relative to the translational frame of reference. Note that $\vec{v}_{rel}$ is non-zero only on the surfaces of the four flaps and is zero on the hull surface. We form a linear system of equations by utilizing equation (4) together with equations (3) and (2). The solution of this linear system, which must be solved at each time step, gives us the strength of the vortex rings that correctly satisfy the boundary condition, equation (4).

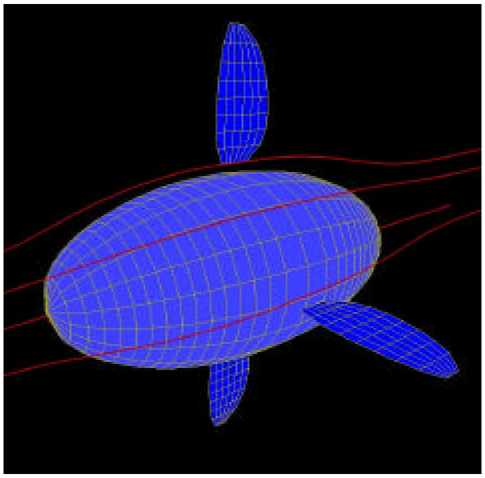

Figure 3 - Model of pilotfish with quadrilateral vortex elements. The figure is shown with streamlines formed by the passing of fluid over the blunt body.

Because the linear system of equations generated by the enforcement of equation (4) at each collocation point produces a system with no unique solution, an additional physical constraint is needed. The Kutta condition, which states that the pressure difference across the trailing edge of each flap is zero,

$$\Delta p_{T.E.} = 0 \tag{5}$$

supplies the added physical constraint that generates a unique solution

In order to solve for the strength of the time-dependent vortex sheet, we use Kelvin's theorem. This theorem states that the time rate change of circulation around a closed loop is zero.

$$\frac{D\Gamma}{Dt} = 0 \tag{6}$$

Using equations (5) and (6), we find the strength of the vortcity shed from each flap.

Efficiency

Efficiency of operation is one of the primary focuses of this model. In order to calculate the cruising efficiency of the pilotfish, we must determine the thrust and power. For steady cruising, the thrust is equal to the drag. We measured the total drag on a scale model of the pilotfish hull in the wind tunnel facilities at Duke University. Using standard similitude, we estimate that the drag produced by the pilotfish cruising in water at $1\,m/s$ to be $27.6\,N$. Therefore, we set in our model a cruising speed of $1m/s$ and a total required thrust equal to our measured drag.

We calculate the efficiency by forming the ratio of input power, P_{in}, to output power

$$e = \frac{P_{in}}{ST} \tag{7}$$

where the output power is the product of cruising speed, S, and average thrust, T. We find the input power by multiplying the torque, Q, by the flap rotation rate, $\dot{\Theta}$

$$P_{in} = \frac{1}{t}\int_{t}^{t+t} Q\dot{\Theta}\,dt \tag{8}$$

where

$$Q = \int_{A} \left(r_s \Delta p\left(\vec{r}\right)\right) dA \tag{9}$$

In equations (8) and (9), t is the period of flap actuation, r_s is the distance from the shaft and $\Delta p\left(\vec{r}\right)$ is the position dependent pressure difference across the thin flap. Note that the area over which we calculate the integral is the area of the four flaps only and not the area of the hull.

The total thrust is specified as part of the problem statement. However, we do not know the actuation amplitude and/or frequency necessary to produce this thrust *a-priori.* Accordingly, we need a method by which to calculate the thrust. We can then adjust either the flap amplitude or frequency until the flaps produce the desired thrust. Typically one can integrate the pressure over a surface to get the total thrust, lift, and side force. In fact in equation (9), we calculate a moment by performing such and integral. While this is a reasonably accurate method for calculating torque, thrust (or drag) calculations can result in significant error. This is due to the "leading edge suction" problem created by our use of a thin plate to approximate the flaps. For more details on this problem and some of the remedies, the reader is referred to Katz & Plotkin (1991).

For the present calculations we compute thrust (or drag) by using the Trefftz volume method discussed by Hall & Hall (1996) and elsewhere. This method utilizes Kelvin impulses to calculate the time averaged thrust produced by the flap propulsors. The thrust/lift/side-force produced by a surface is a direct result of the increase in momentum of the surrounding fluid. The Trefftz volume model uses that fact that the change in momentum over one period of oscillation can be obtained from the momentum contained in the wake over one period. In order to avoid start-up effects, we allow the flaps to actuate for enough time so that the initial transients no longer have any significant effect on the power and thrust calculations.

Our derivation of thrust calculations follow that of Hall & Hall (1996). We begin with the linear momentum, $\vec{x}$, deposited in the wake by one period of flap actuation

$$\vec{x} = r \iiint_V \nabla\Phi dV \qquad (10)$$

where the volume V encloses one period of shed vorticity. Next we use Gauss' divergence theorem to transform the volume integral into a surface integral where the surface of integration, A, is the surface, with outward-pointing unit normal $\hat{n}$, of the volume bounding V.

$$\vec{x} = -r \iint_A \Phi\hat{n}dA \qquad (11)$$

Because of the periodic structure of the wake, the integral cancels everywhere except on the wake sheet itself. Therefore, our surface integral becomes

$$\vec{x} = -r \iint_W \Delta\Phi\hat{n}dA = -r \iint_W \Gamma\hat{n}dA \,. \qquad (12)$$

In writing equation (12), we have made use of the fact that for these vortex rings

$$\Gamma = \Delta\,\Phi = \Phi_{upper} - \Phi_{lower}\,. \qquad (13)$$

The average force per cycle of actuation is

$$\vec{F} = -\frac{\vec{x}}{t} = \frac{r}{t} \iint_W \Gamma\hat{n}dA. \qquad (14)$$

We form the dot product with the direction of interest in order to get the component of force in that direction. In this case, the thrust is

$$F_x = \frac{r}{t} \iint_W \Gamma \hat{i} \cdot \hat{n} dA. \qquad (15)$$

By using this Trefftz calculation method for thrust computations, we avoid the "leading edge suction" inaccuracies.

Wake Distortion

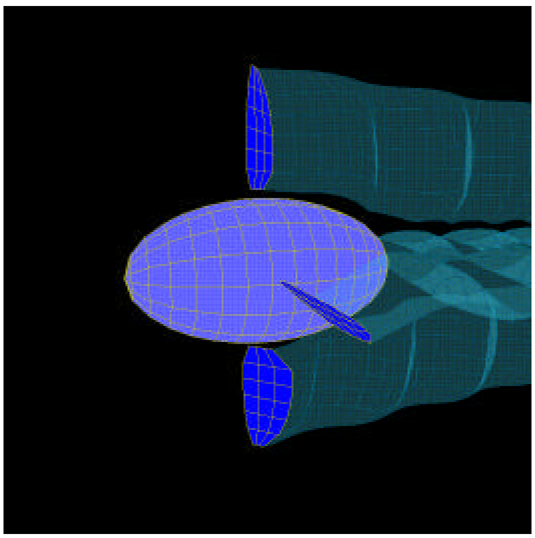

Figure 4 - Vortex shedding from Pilotfish flap propulsors. This image clearly shows the stretching of the vortex sheets as they convection past the blunt aft end of the hull.

In this section we give a brief discussion of the distortion of the wave sheet in the region of space just behind the pilotfish hull. Figure 4 shows the distortion of the wave sheet shed from the propulsors. Note that the stretching is non-uniform. For example the lower portion of the sheet shed form the top flap deforms more than the upper portion. Hall & Hall (1996) found that there exists an optimal distribution of vorticity on the wake sheet for flapping flight. Their situation was a bit simpler that the problem considered here. In order for the vorticity distribution in the wake to have the optimal distribution, we must change the shape of the propulsor from the geometry optimized in the absence of the blunt hull.

Conclusion

In this paper we have discussed the whole-vehicle simulation of propulsion by undulatory flap actuation of a prototype UUV. Our numerical method makes use of an unsteady vortex ring technique. These results of this calculation show that flow perturbation effects of bluff bodies needs to be properly accounted for in the design of flap propulsors.

This numerical model will serve as the basis for a multi-parameter optimization of flap propulsors. The parameters we plan to investigate include flap planform, actuation cycle, chord-wise placement of the actuation shaft and input actuation wave shape. Since the required thrust is known *a-priori*, our optimization output will produce an actuation cycle producing that thrust but with maximum efficiency.

Acknowledgments

This project is sponsored by the Office of Naval Research through grant #N00014-99-1-0452. We would also like to acknowledge our on-going collaboration with Nekton Research, LLC involving this and related projects.

References

Anderson, J.M. and Kerrebrock. P.A. (1997) The Vorticity Control Unmanned

Undersea Vehicle (VCUUV) An Autonomous Vehicle Employing Fish Swimming Propulsion and Maneuvering. *Proceedings of the 10th International Symposium on Unmanned Untethered Submersible Technology*. Autonomous Undersea Systems Institute, Lee, NH.

Anderson, J.M., Streitlien, K., Barrett, D.S., Triantafyllou, M.S. (1998) Oscillating Foils of High Propulsive Efficiency, *J. Fluid Mech.*, vol. 360, pp. 41-72.

Dickinson, M.H. (1994) The Effects of Wing Rotation on Unsteady Aerodynamic Performance at Low Reynolds Numbers, *J. Exp. Biol.* vol. 192, pp.179-206.

Hall, K.C. and Hall, S.R. (1996) Minimum Induced Power Requirements for Flapping Flight, *J. Fluid Mechanics* vol. 323, pp. 285-31.

Hobson, B., Murray, M., Pell, C. (1999) Pilotfish: Maximizing Agility in an Unmanned-Underwater Vehicle *Proceedings of the 11th International Symposium on Unmanned Untethered Submersible Technology*. Autonomous Undersea Systems Institute, Lee, NH.

Kagemoto, H., Wolfgang, M.J., Yue, D.K.P., Triantafyllou, M.S. (2000) Force and Power Estimation in Fish-Like Locomotion Using a Vortex Lattice Method, *J. Exp. Biol.*, vol. 122, pp. 239-253.

Katz, J. and Plotkin, A. (1991) *Low Speed Aerodynamics*. McGraw-Hill, Inc., NY.

Murray, M.M. and Howle, L.E. (2001) Spring Stiffness Influence on an Oscillating Propulsor *J. of Fluids and Struct*., Accepted for publication.

Sfakiotakis, S., Lane, D.M., and Davies, B.C. (1999) Review of Fish Swimming Modes for Aquatic Locomotion, *IEEE J. Oceanic Eng.*, vol. 24, pp.237-252.

Triantafyllou, M.S., Triantafyllou, G.S., Yue, D.K.P. (2000) Hydrodynamics of Fish-Like Swimming, *Annu. Rev. Fluid Mech.*, vol. 32, pp. 33-53.